Automatic alignment of a displacement-measuring heterodyne interferometer

Jennifer E. Logan Peter G. Halverson Martin W. Regehr
Robert E. Spero

26 September 2001
Revised 8 April 2002

Abstract

A technique for automatically aligning the beams of displacement-measuring interferometric gauges is described. The pointing of the launched beam is modulated in a circular pattern and the resulting displacement signal is synchronously demodulated to determine the alignment error. This error signal is used in a control system that maintains the alignment for maximum path between a pair of fiducial hollow-cube corner retroreflectors, hence minimizing sensitivity to alignment drift. The technique is tested on a developmental gauge of the type intended for SIM, the Space Interferometry Mission. The displacement signal for the gauge is generated in digital form, and the lock-in amplifier functions of modulation, demodulation, and filtering are all implemented digitally.

1 Introduction

SIM, the Space Interferometry Mission[1, 2], is an orbiting stellar interferometer planned for launch in 2009. It has a target astrometric accuracy of approximately 10^{-11} radian. A key element of SIM is a cluster of displacement-measuring heterodyne interferometer gauges[4, 3, 5] that monitor changes in the separation of telescope mirrors. These gauges must be linear and repeatable to approximately 10 picometer (pm) as the optical paths change by as much as 1 m. One source of astrometric error is inaccuracy or drift in the orientation of the optics that launch the $\lambda = 1.319$ micron wavelength laser beam[6]. The optics will be mounted on the spacecraft structure, which may have a deployment error on the order of 1 milliradian and be unstable at the level of 10 microradian. We describe a control system designed to sense and reduce initial error and drift to approximately 10 microradian and 1 microradian, respectively—the levels needed to meet the overall gauge requirement.

The control system uses mechanical modulation of the launch angles (θ, ϕ) and synchronous demodulation of the path-length output of the gauge (the well-known lock-in amplifier technique). It is similar to previous investigations based on modulation to align the mirrors of Fabry-Perot cavities[7]. Since the SIM gauges generate their output in digital form, we implement the lock-in amplifier digitally, and use digital filters for the control system.

2 Control System

2.1 Effect of Beam Tilt

The measurement of interest is the optical path between a pair of fiducial hollow-cube corner retroreflectors. As shown in Figure 1 for the two-dimensional case of roof retroreflectors, this path length is insensitive to changes in the retroreflector angle, as well as to translation of the retroreflector perpendicular to the beam direction.

A two-dimensional (roof) retroreflector is shown (*heavy line*) tilted with respect to the launched beam *xb*. The tilt angle is α. Since *bca* is a right angle, the reflected beam *az* is parallel to *xb*, and both are perpendicular to the line of interference, *xz*. We seek to demonstrate that the length of path *xbaz* is equal to *ycy*; the latter path is by construction independent of α. The three angles at *a* labeled α are equal, which implies that triangles *abc* and *acd* are congruent, and that $bc = cd$ and $ab = ad$. Now from the similar triangles bcf and bde, with $bc = cd$, we have $ed = 2fc$, and we see that $xb + ba + az = 2(yf + fc)$, as required. This equality holds for arbitrary rotation angle α and transverse translation bf.

That is, the measured distance between a retroreflector and a reference plane perpendicular to the direction of propagation of the beam depends only on the shortest distance between the retroreflector vertex and the plane. This result generalizes to three dimensions[8], where the tilt can be out of the plane of the figure, and the retroreflector is a cube corner instead of a roof.

For two cube corners, as the launch angle changes away from parallel to the line joining the vertices of the two cube corners, the reference plane rotates so that the two perpendicular distances become shorter, and the measured distance between two corner cubes decreases. Figure 2 explains this behavior in two dimensions.

The launcher is shown as the dark-lined, boxed, **L**-symbol. The distance between fiducial reflectors is L_0. Sub-figure *(A)*: After striking the right reflector and returning to the the plane of launch, the image of the launcher is inverted (short dashed lines). *(B)*: The beam returns to the launcher after reflecting from the left reflector (solid line path between reflectors). The upright image has traveled $2L_0$ (short dashed line to left of left reflector). When the launched beam is tilted by θ with respect to the line joining the reflector vertices, the beam follows the path of the long-dashed line. The misalignment by θ corresponds to the launcher image being tilted by θ; this is represented by the tilted wavefront in *(C)*. The approximation of a nearly-parallel wavefront is valid, since the displacement due to misalignment *bc* is small compared to the spot radius. The distance $2L$ that the wavefront travels before reaching the aperture at *c* is shortened relative to the distance $2L_0$ that an aligned wavefront would travel: $2L = 2L_0 \cos\theta$. This implies the well-known result[4] that if the launch angle deviates by θ from the line to the vertex, the measured path changes by $L = L_0 \cos\theta$, where L_0 is the distance to the vertex[9]. Since θ is small, length changes can be approximated by $\Delta L \approx -(L_0/2)\theta^2$.

The dependence on θ was verified by scanning the launch angle by as much as $2 \cdot 10^{-4}$ radian in two axes, and simultaneously monitoring the gauge output (Figure 3). Considering the alignment error as composed of static misalignment θ_0 and a fluctuation $\Delta\theta$, path changes can be approximated by

$$\Delta L = -L_0 \theta_0 \Delta\theta. \tag{1}$$

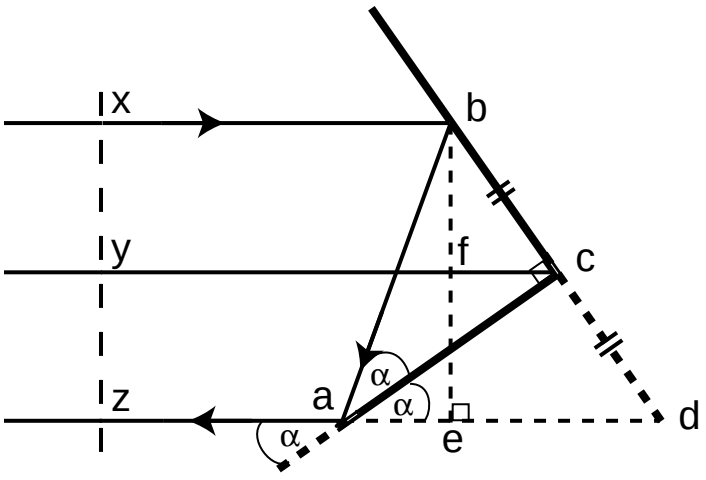

Figure 1: Path-length insensitivity to reflector angle α and lateral translation bf.

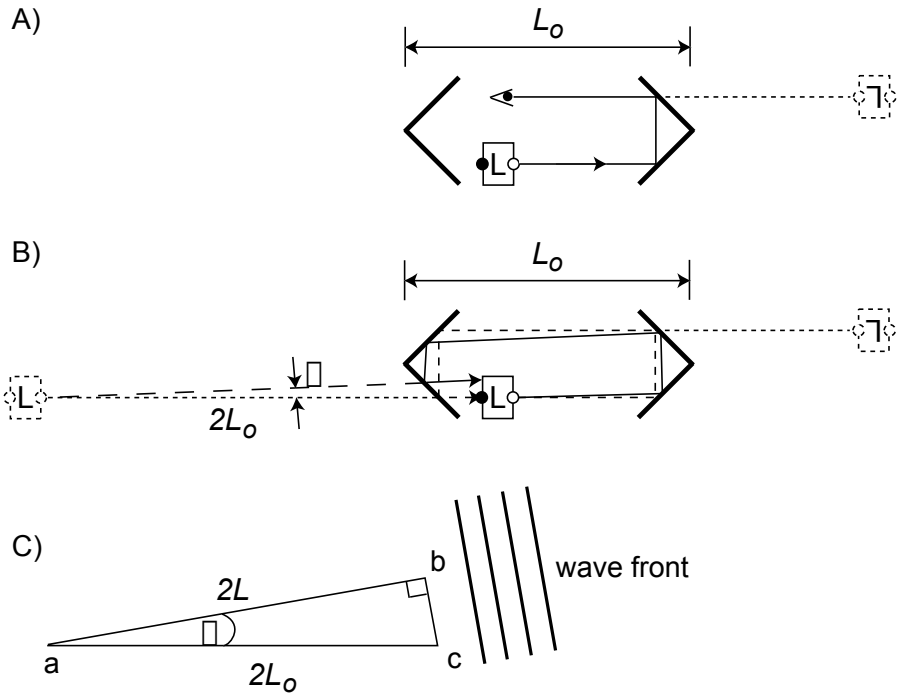

Figure 2: The dependence of pointing error on $\cos\theta$.

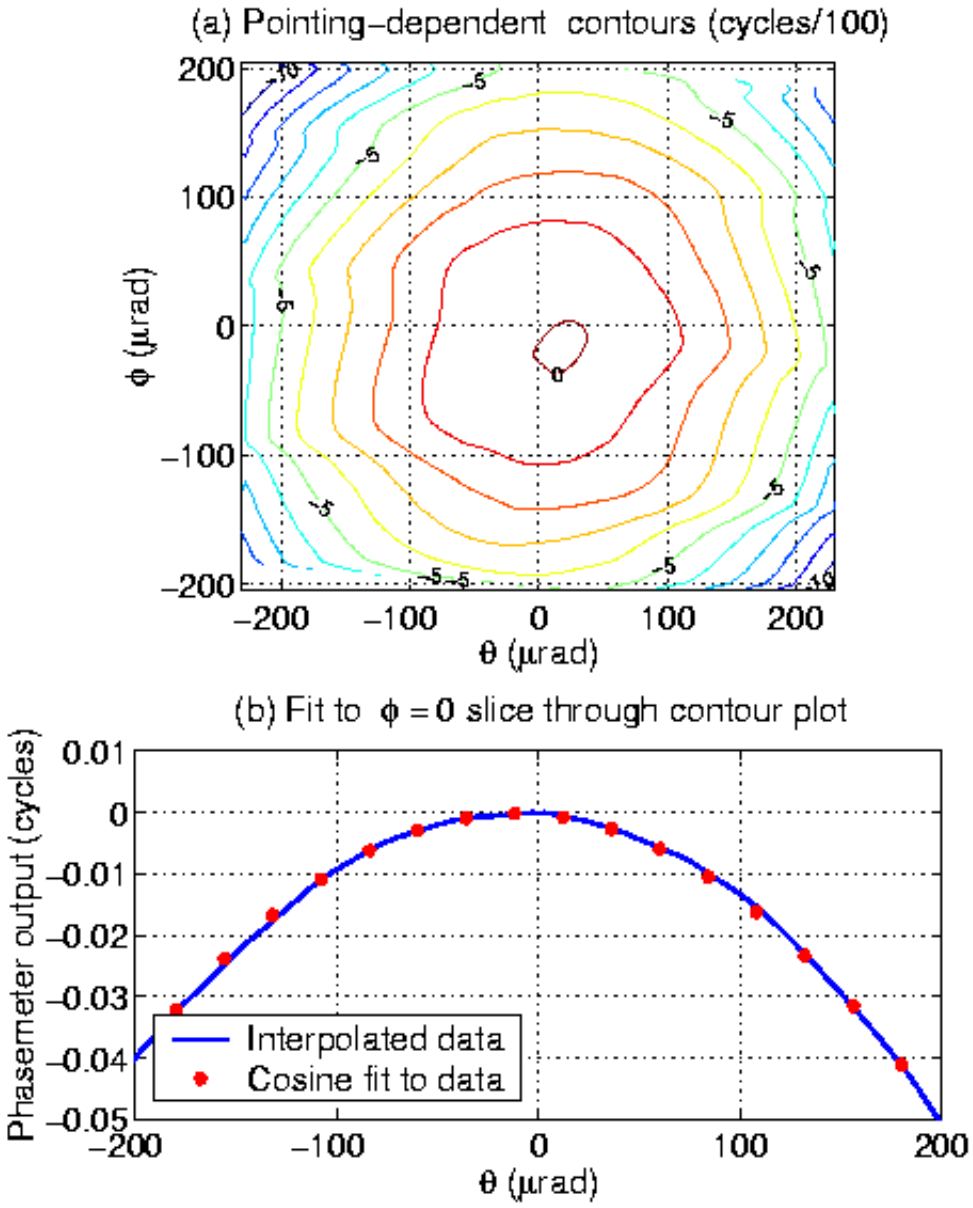

Figure 3: Measured optical path in response to variation of launch angles. *(a):* Contours of equal optical path, as a function of the tip/tilt launcher angles θ and ϕ. The contours are spaced by 0.01 cycles of phase, or 6.6 nm. *(b):* The $\phi = 0$ slice through the data in *a*, and the calculated cosine-dependence of optical path on θ.

2.2 Implementation of control

In addition to specifying the error for given static and dynamic misalignments, Equation (1) forms the basis for measuring the misalignment. The pointing is intentionally modulated by $\Delta\theta$, and the measurement system responds with signal ΔL, proportional to misalignment θ_0.

The modulation and control system is shown in Figure 4. A pointing actuator modulates the beam in a circular pattern at 2.5 Hz, with diameter 60 microradian.

(For simplicity, the diagram includes only one of the two controlled degrees of freedom.) This actuator uses three PZT elements forming a triangle with spacing of 39 mm between the elements that actuate in the θ direction, and 29 mm in the ϕ direction. A software conversion matrix scales the voltages to provide the circular modulation pattern. The fiducial cube corners are separated by 70 cm. The interferometer beam executes a round trip and is interfered with the launched beam; the interference is detected on a photodiode. Length measurement is based on the heterodyne technique: A 100 kHz frequency shift between the launched beam and a reference beam imposes an interferometric phase shift on the detected signal[4] that is proportional to the length traversed by the beam. The phase-meter[10] consists of analog filters and specialized digital hardware that converts the phase shift into displacement, generating a digital signal proportional to the path length x. The two tilt angles θ and ϕ are detected separately by demodulating in-phase (shown) and in quadrature (not shown). The quadrature-phase control is the same as for in-phase control; the error signal is derived by shifting the reference oscillator by 90 degrees relative to the multiplication.

The block enclosed within the dashed lines is a digital lock-in amplifier. It contains the following software elements:

1. A sine-wave generator that supplies modulation of amplitude x_A at 2.5 Hz.
2. A high-pass digital filter G_{HP} to eliminate the D.C. component of x.
3. Demodulation by multiplication of x by the sinusoidal modulation. The output of the multiplier, x_M, is the error signal.
4. A low-pass digital filter G_{LP} and gain multiplier G. The correction signal $x_G = x_M G G_{LP}$.

A digital-to-analog converter (DAC) and high-voltage amplifier drive the piezoelectric actuator (PZT) with the sum of the correction signal and modulation.

2.3 Control system parameters

Since the modulation and correction are at frequencies below the first mechanical resonance of the system, the frequency-dependence is expected to be contained entirely in the single-pole low-pass filter. That is, the open-loop gain[11] is

$$GH = \frac{k}{1+s\tau}, \tag{2}$$

where k is a constant set by the software and hardware gains, s is the laplace variable, and τ is the filter time-constant. The closed-loop gain is

$$C(s) = \frac{GH(s)}{1+GH(s)}, \tag{3}$$

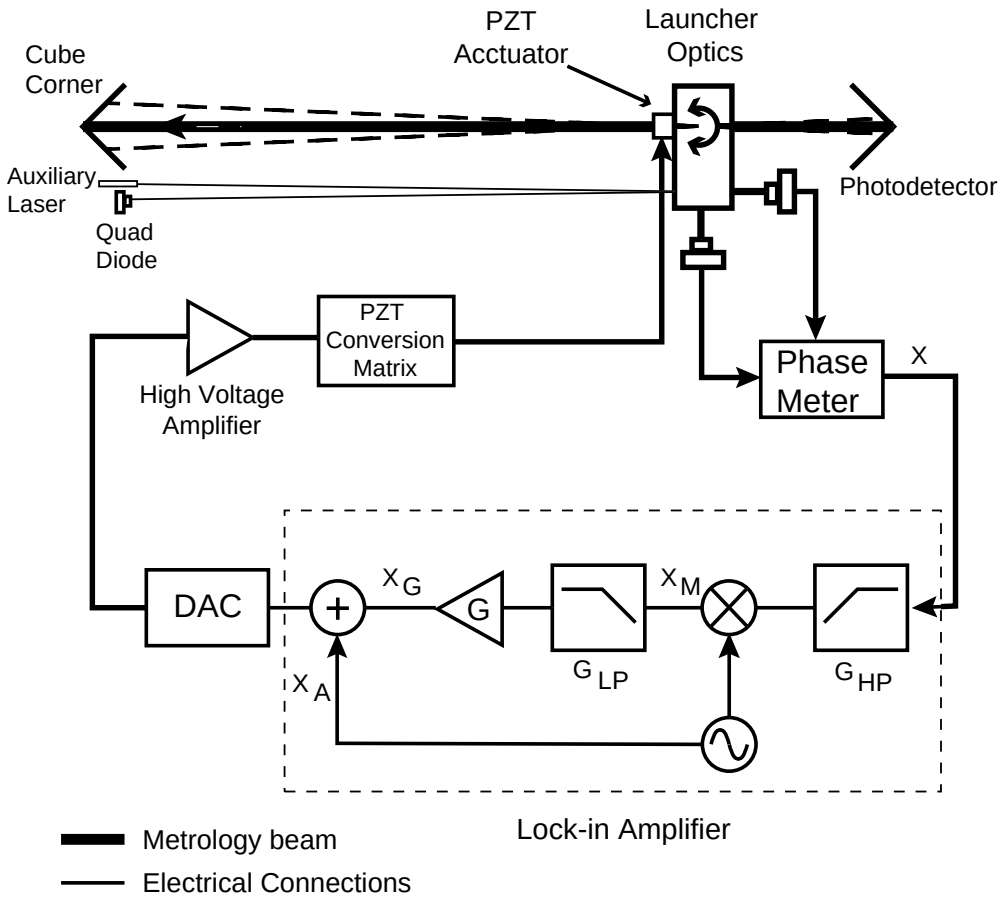

Figure 4: Control system for alignment of metrology beams to cube-corner vertices. (One of two controlled axes shown). Thin and medium lines represent digital and analog signals, respectively. The phase-meter measures the phase difference between two photodiode signals: one that detects the interfered beam that has traversed the path between the corner cubes (signal), and one that detects the short-path interference within the launcher optics (reference). The laser diode transmitter and quadrant photodidode receiver provide an out-of-loop monitor of control system performance.

The closed-loop impulse response is the inverse laplace transform of $C(s)$. The quantity of interest for comparison with measurements is the closed-loop step response $p(t)$, which is the inverse laplace transform of $C(s)/s$. For a unit step:

$$p(t) = \frac{k}{1+k}\left(1 - \exp(-\frac{(1+k)t}{\tau}\right) \tag{4}$$

The gain was varied under software control within the range $10 < k < 200$. The expected drifts on SIM require $k \geq 10$.

3 Performance and comparison with requirements

The performance of the control system was measured by an optical lever consisting of an external laser 52 cm from the launcher that strikes a mirror affixed to the launcher housing, and a quadrant photodiode adjacent to the laser that intercepts the reflected beam. The processed quadrant photodiode signal provides a measure of the launcher pointing that is independent of the controlled signals.

Figure 5 shows the control system response to an imposed step disturbance in the launcher pointing.

The optical lever θ signal records the transient response and recovery, and the θ correction signal (x_G in Figure 4) shows the step change in voltage required to track the cube corner position. For this test, the filter time constant was $\tau = 1.6 \cdot 10^3$ sec, and the gain was $k = 200$. The launcher pointing angle returned to within 1% of the imposed disturbance, consistent with the noise level and prediction of Equation 4. The large value of τ implements a control law that is equivalent to an integrator at most time-scales of interest. A valid error signal is produced even if the gauge is initially misaligned by an amount much larger than the modulation amplitude—the acquisition range is limited only by the range of the PZT angle actuators, approximately 500 microradian.

The long-term performance is indicated in Figure 6. The peak-to-peak drift over 40 hours, as measured by the optical lever, was 8 microradian.

This is to be compared with the SIM requirement of average variation not to exceed 1 microradian over times of approximately 1 hr. The launch angle of the optical lever was shown in separate measurements to drift by an amount approximately the same as the observed drift, so we conclude that the measured drift is an upper limit. Demonstrating the required stability will require improving the optical lever performance, possibly by improved thermal stabilization. In addition to the drift, a relatively high-frequency variation in pointing angle is imposed by the control system. This variation is sinusoidal in the measured optical-path x, with frequency $2x/\lambda$ and peak-to-peak amplitude of approximately 3 microradian; the mechanism is under investigation. Future experiments with multiple gauges will test the absolute pointing requirement of 10 microradian.

Acknowledgements

Frank Loya provided essential support in developing the final version of the control and data collection software. This research was performed at the Jet Propulsion Laboratory, California Institute of Technology, under a contract to the National Aeronautics and Space Administration.

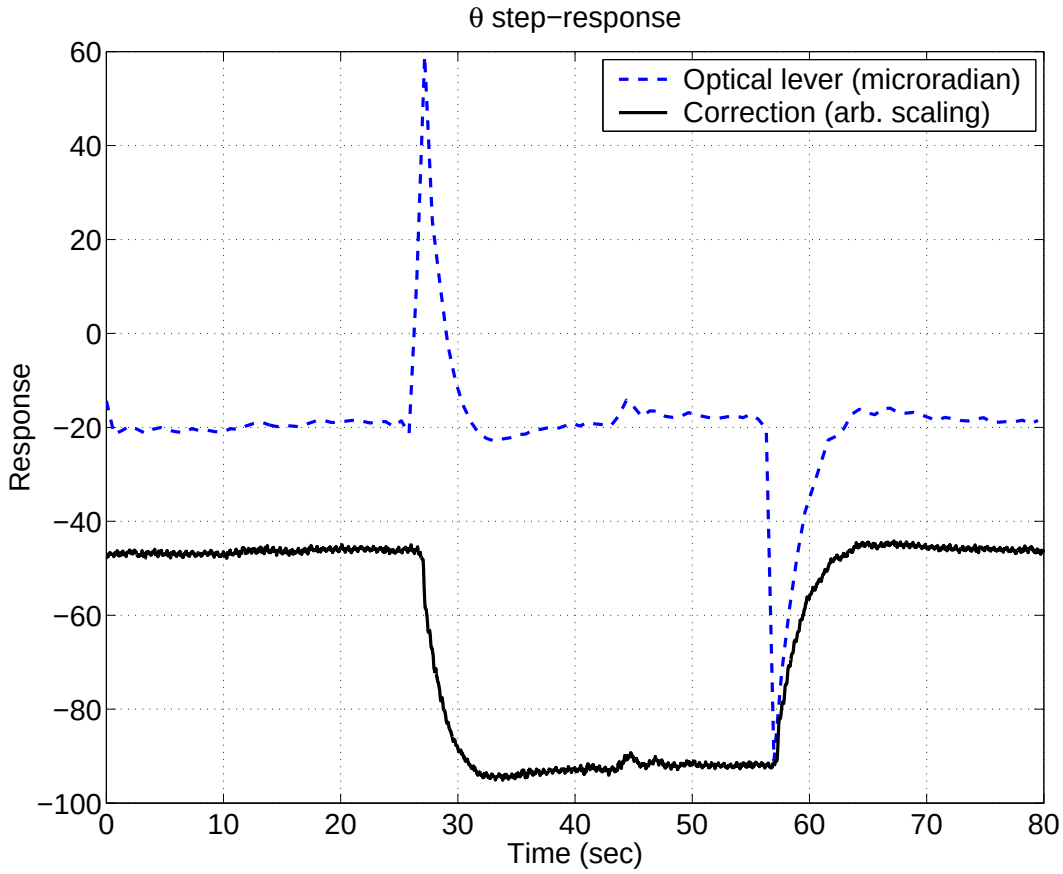

Figure 5: Step response of the pointing control system. The dashed line is the optical lever response, and the solid line is the correction signal. At $t = 27$ sec, a disturbance of 80 microradian was injected by applying a step change in the PZT actuator voltage. At $t = 55$ sec, a similar disturbance was applied in the opposite direction.

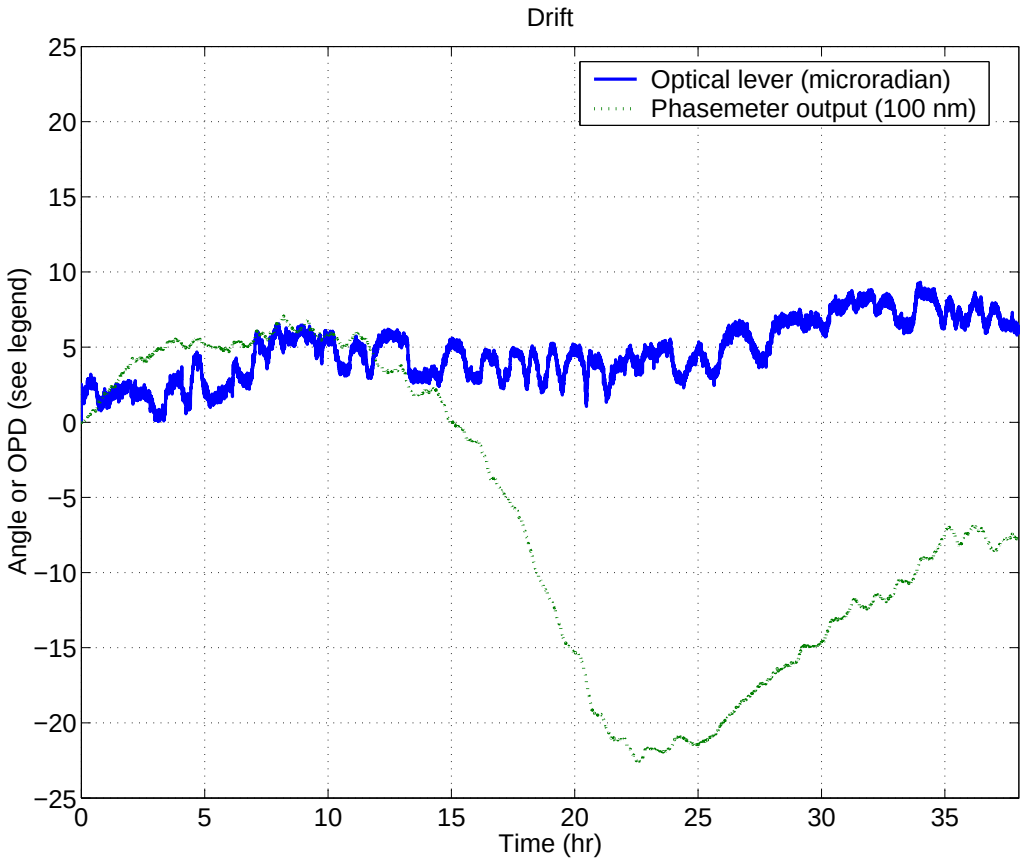

Figure 6: Long-term stability of beam pointing. The solid trace is is the optical lever response, and the dotted trace is the phsemeter output measurement of the optical path change.

References

[1] http://sim.jpl.nasa.gov.

[2] T Boker and RJ Allen. "Imaging and nulling with the Space Interferometer Mission". *Ap J Supp*, 125(1):123–142, 1999.

[3] Shigeru Hosoe. "Highly precise and stable displacement-measuring laser interferometer with differential optical paths." *Precision Engineering*, 17:258–265, 1995.

[4] N. Bobroff. "Recent advances in displacement measuring interferometry." *Meas. Sci. Technol.*, 4:907–926, 1993.

[5] Koichiro Miyagi, Massaya Nanami, Isao Kobayashi, and Akira Taniguchi. "A compact optical heterodyne interferometer by optical integration and its application." *Optical Review*, 4(1A):133–137, 1997.

[6] S. Shaklan, S. Azevedo, R. Bartos, A. Carlson, Y. Gursel, P. Halverson, A. Kuhnert, Y. Lin, R. Savedra, and E. Schmidtlin. "Micro-Arcsecond Metrology testbed (MAM)," in *SPIE Proceedings on Astronomical Interferometry*, Robert D. Reasenberg, editor, Harvard-Smithsonian Ctr. for Astrophysics, Cambridge, MA. Proc. SPIE 3350,100–108, 1998. Abstract and ordering information available at http://www.spie.org/web/abstracts/3300/3350.html.

[7] K. Kawabe, N Mio, and K Tsubono. "Automatic Alignment-control system for a suspended Fabry-Perot cavity." *Appl Opt*, 33(24):5498–5505, 1994.

[8] P. Haschberger and O. Mayer. "Ray tracing through an eccentrically rotating retroreflector used for path-length alteration in a new Michelson interferometer." *J. Opt. Soc. Am. A*, 8(12):1991–2000, 1991.

[9] In addition to this geometric error, there are errors associated with imperfections in the optics, including non-planar reflecting surfaces, corner gaps, and departures from perfect orthogonality of the surfaces. The latter may be the most significant; if there is a "dihedral error" ε deviation from 90 degrees in the orientation of the cube corner faces, Equation (1) becomes $\Delta L = L_0\theta_0(\Delta\theta + 2\varepsilon)$. For high-quality retroreflectors, $\varepsilon \approx 5$ microradian.

[10] P. Halverson, D. Johnson, A. Kuhnert, S.Shaklan, and R. Spero. "A multichannel phasemeter for picometer precision laser metrology." *Proc. SPIE Conf on Optical Engineering for Sensing and Nanotechnology (ICOSN '99)*,I. Yamaguchi, editor, 3740:646–649, 1999.

[11] Richard C. Dorf and Robert H. Bishop. *Modern Control Systems*. Prentice-Hall, 2001.